Acta Cryst. (1993). A**49**, 655–661

On the Modelling of Neutron Diffraction Reflections from Small Single Crystals

BY A. MCL. MATHIESON

Division of Materials Science and Technology, CSIRO, Clayton, Victoria 3168, *Australia, and Chemistry Department, La Trobe University, Bundoora, Victoria* 3083, *Australia*

AND A. W. STEVENSON

Division of Materials Science and Technology, CSIRO, Clayton, Victoria 3168, *Australia*

(*Received* 1 *September* 1992; *accepted* 27 *January* 1993)

Abstract

For the case where the rotation axis of the monochromator crystal and that of the small specimen crystal are parallel, *i.e.* (+, −) or (−, +) configuration, the apparatus function in two-dimensional $\Delta\omega$, $\Delta 2\theta$ space is associated with the source, *S*, the monochromator crystal, *M*, and an idealized specimen crystal, *c*, which is vanishingly small and has zero mosaic spread. For any value of t ($=\tan\theta_c/\tan\theta_M$), the apparatus function is a *product* of the distributions (with their respective loci of translation) of: (i) the emissivity of *S*; (ii) the reflectivity over the length of *M*; (iii) the mosaic spread of *M*; and (iv) the wavelength band arising from the vector addition in $\Delta\omega$, $\Delta 2\theta$ space of the wavelength dispersion of *M* and of *c*. To combine the apparatus function with other components such as the mosaic spread of a real specimen crystal, its physical dimension, the size of the aperture in front of a quantum detector or the point-spread function of a position-sensitive detector, the appropriate mathematical operation in $\Delta\omega$, $\Delta 2\theta$ space is *sequential convolution*. Examples are given, for $t = 0$ (0.25) 1.0 (0.5) 2.0, of synthetic apparatus functions based on typical dimensions appropriate to neutron diffraction experimental arrangements. These are presented in $\Delta\omega$, $\Delta 2\theta^{(0)}$ space, which corresponds to ω-scan data collection. The advantage of modifying these by affine transformation to $\Delta\omega$, $\Delta 2\theta^{(2)}$ space or, equivalently, to correspond to ω–2θ-scan data collection, is demonstrated.

Introduction

To obtain physically significant estimates of structure factors from measurement of the intensity of Bragg reflections from a small single crystal, *c*, it is a basic requirement to be able to establish, for each reflection, a suitable two-dimensional region in diffraction space [see Mathieson (1988*a*) and Mathieson & Stevenson (1985)] within which the intensity measurement is to be made, in order to ensure that consistent truncation limits (Denne, 1977) are selected.

To do this, one needs to find a way of determining the distribution of the diffracting power of reflections, referred to colloquially as its shape, as the scattering angle, θ_c, changes. Two approaches have been taken in neutron diffractometry involving a monochromator.

One approach is empirical, in that it examines the more intense reflections over the range of scattering angles and uses these to determine the effective shape in any given region of θ_c. This knowledge is then utilized to deal with the weaker reflections nearby and to govern decisions on the measurement limits of these less well defined cases. Early exponents were Spencer & Kossiakoff (1980) and Sjölin & Wlodawer (1981) and variants of this approach were presented in preliminary form at a meeting on the position-sensitive detection of thermal neutrons (Convert & Forsyth, 1983). Latterly, more detailed accounts have been presented by Wilkinson, Khamis, Stansfield & McIntyre (1988) and Lehmann, Kuhs, McIntyre, Wilkinson & Allibon (1989). However, as we have noted (Mathieson, 1988*a*), there are limitations to this *ad hoc* approach, particularly as one progresses to higher angles and the population of intense reflections falls while the uncertainties as to what should constitute the truncation limits increase. Moreover, evidence that the method of analysis chosen may lead to systematic differences has been noted by Stansfield, Thomas, Mason, Nelmes, Tibballs & Zhong (1983).

The other approach is to simulate the shapes of the reflections on the basis of a theoretical model. This approach was first explored in respect of neutron diffractometry by Schoenborn (1983), for protein-crystal studies. Later, an *ab initio* examination was made by Mathieson (1988*a*), to identify the contributions of the various physical factors to the reflection shape and how, as a result, the reflection shape in $\Delta\omega$, $\Delta 2\theta$ space changed with $\theta_c^{(0)}$.* The primary role

* To identify the magnitude of the $\Delta 2\theta$ offset ($=n\Delta\omega$) for each step in $\Delta\omega$ involved in affine transformation of $\Delta\omega$, $\Delta 2\theta^{(0)}$ space, the terminology, $\Delta\omega$, $\Delta 2\theta^{(n)}$ has been used (Mathieson, 1983). Where no identifying superscript appears, $\Delta\omega$, $\Delta 2\theta^{(0)}$ is to be understood.

ISSN 0108-7673

of the parameter t ($=\tan\theta_c/\tan\theta_M$) was noted earlier in relation to two-dimensional reflection shapes (Mathieson, 1985) and its key influence in determining shape was later stressed in Mathieson (1988*a*). To make the influence of individual contributions more obvious, square and triangular functions were used rather than smooth functions such as Gaussians. Provided one establishes a physically realistic model, one should be in a position to set consistent measurement and truncation conditions over the whole working range of θ_c even where there are few or no strong reflections.

Stevenson (1989) has explored the simulation of reflection shapes by a different procedure and in greater detail than Mathieson (1988*a*). His procedure was to trace the rays from a given point in $\Delta\omega, \Delta 2\theta$ space back *via* the idealized (zero-mosaic, point) specimen crystal and the monochromator crystal to the source and thus generate the shape in $\Delta\omega, \Delta 2\theta$ space associated with specific parameters of the components. Within this approach, he has given mathematical expression for the variation of the shape due to components of different magnitudes for any given value of t.*

Since the publication of our respective papers [Mathieson (1988*a*) and Stevenson (1989), which we refer to from now on as *M*88 and *S*89, respectively], we have, more recently, been considering the compatibility of our two approaches. In the process, we have come to realize that the situation under review is somewhat more subtle than it had first appeared; that, in two-dimensional diffraction space, not all components in the overall experiment are functionally equivalent. For the combination of the various components, one has to ensure that the mathematical operation chosen to effect combination is compatible with the physical operation involved.

In the present case, it turns out that the basic question is when does one use convolution and when does one not?

Differentiation of components

In Alexander & Smith's (1962) modelling of one-dimensional profiles of Bragg reflections, the mode of combination of all components was the same. The final profile was attained by sequential convolution, *vide* equation (1) of Alexander & Smith (1962). The actual sequence of combination of the components did not matter; the end result was the same.

On close examination of the details of combining components in two-dimensional $\Delta\omega, \Delta 2\theta$ space in the case where the axes of the monochromator crystal and that of the specimen crystal are parallel, *i.e.* the $(+,-)$ and $(+,+)$ configurations, we find that this generality does not hold. The components fall into two classes with different modes of combination, so the sequence of combination is restricted.

1. *The basic components of the apparatus function*

The elements that require careful scrutiny are those that are involved in the apparatus function as we define it here (see Appendix), namely, the source, *S*, the monochromator crystal, *M*, and the idealized specimen crystal, *c*, whose prime role in respect of the apparatus function is to provide dispersion and which, at this stage, is considered to be vanishingly small and to involve zero mosaic spread. The components of the apparatus function are the four distributions associated with the emissivity of *S*, the variation of reflectivity along the length of *M*, the mosaic spread of *M* and the wavelength band arising from the interaction of the wavelength dispersion of *M* and of *c*.

Examination of the change of shape in terms of t initially is too general and therefore not very instructive. It is advisable to focus on a specific value of t (say 0.4) and to explore the effect of the various components on the overall shape. The situation for other values of t can then be identified and followed through.

The contributions of the various components to the overall shape of the apparatus function are introduced as follows [$t=0.4$]:

(*a*) *The length of the monochromator crystal.* When the length of the monochromator crystal in the plane of diffraction is set as (say) $M_+M_0M_-$ (see Fig. 1 in *M*88), this establishes the reference line, 0′00″ for $\theta_c=0°$ in Fig. 1(*a*). It also establishes the lower and upper bounds, $Z'_-0'Z'_+$ and $Z''_-0''Z''_+$, respectively, indicated by the dashed lines at a slope of arctan(1/2) to the $\Delta 2\theta$ axis. The locus of translation of the reflectivity distribution along the monochromator is parallel to these lines. Assuming that the reflectivity of *M* is uniform across its surface, it can be represented by a rectangular distribution of unit height and length m_1m_2, which falls to zero outside the upper and lower bounds (see r_M in Fig. 1*a*).

(*b*) *The length of the source.* In respect of the source contribution, it has been shown in *S*89 that one has to take into account not only the value of t but also the distance between *S* and *M*, d_1, and that between *M* and *c*, d_2. For values of d_1 and d_2 appropriate to neutron sources, such as 3.5 and 1.5 m,

* Following the convention of Allison & Williams (1930), for the $(+,-)$ configuration, Mathieson (1985, 1988*a*) nominated t values as negative. To avoid the mathematical problems associated with negative θ, Stevenson (1989) nominated t values as positive. In the present text, we use the latter convention. The problem of a suitable nomenclature is not straightforward, being linked to the particular viewpoint adopted (see DuMond, 1937).

respectively, the locus of translation in $\Delta\omega$, $\Delta 2\theta$ space of the centre point of the source corresponds to a line at $\sim 50°$ to the $\Delta 2\theta$ axis [see equation (17) in *S*89].*

So, for a source length S_1S_2 (say), symmetric about the centre point S_0, this corresponds to a band s_1s_2 in $\Delta\omega$, $\Delta 2\theta$ space, indicated by dotted lines in Fig. 1(*a*). Again, the emissivity may be depicted by a rectangular distribution (if the emissivity is uniform) of length s_1s_2 falling to zero outside the band (see e_S in Fig. 1*a*).

* In a strict sense, the slope for points on the source other than the centre differs to a very minor extent from that at the centre [see equation (17) in *S*89]. Generally, the difference can be ignored.

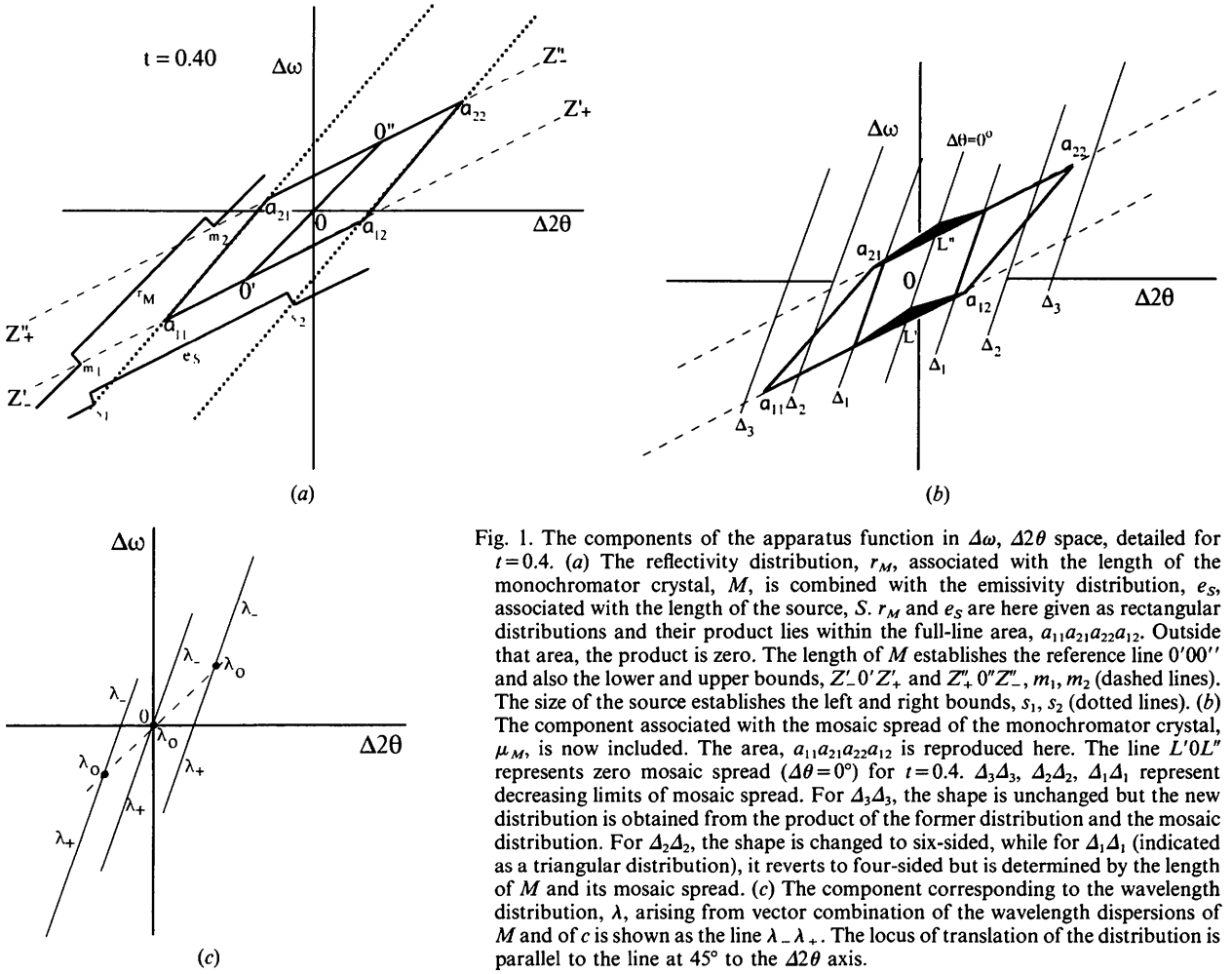

Fig. 1. The components of the apparatus function in $\Delta\omega$, $\Delta 2\theta$ space, detailed for $t=0.4$. (*a*) The reflectivity distribution, r_M, associated with the length of the monochromator crystal, M, is combined with the emissivity distribution, e_S, associated with the length of the source, S. r_M and e_S are here given as rectangular distributions and their product lies within the full-line area, $a_{11}a_{21}a_{22}a_{12}$. Outside that area, the product is zero. The length of M establishes the reference line $0'00''$ and also the lower and upper bounds, $Z'_-0'Z'_+$ and $Z''_+0''Z''_-$, m_1, m_2 (dashed lines). The size of the source establishes the left and right bounds, s_1, s_2 (dotted lines). (*b*) The component associated with the mosaic spread of the monochromator crystal, μ_M, is now included. The area, $a_{11}a_{21}a_{22}a_{12}$ is reproduced here. The line $L'0L''$ represents zero mosaic spread ($\Delta\theta=0°$) for $t=0.4$. $\Delta_3\Delta_3$, $\Delta_2\Delta_2$, $\Delta_1\Delta_1$ represent decreasing limits of mosaic spread. For $\Delta_3\Delta_3$, the shape is unchanged but the new distribution is obtained from the product of the former distribution and the mosaic distribution. For $\Delta_2\Delta_2$, the shape is changed to six-sided, while for $\Delta_1\Delta_1$ (indicated as a triangular distribution), it reverts to four-sided but is determined by the length of M and its mosaic spread. (*c*) The component corresponding to the wavelength distribution, λ, arising from vector combination of the wavelength dispersions of M and of c is shown as the line $\lambda_-\lambda_+$. The locus of translation of the distribution is parallel to the line at 45° to the $\Delta 2\theta$ axis.

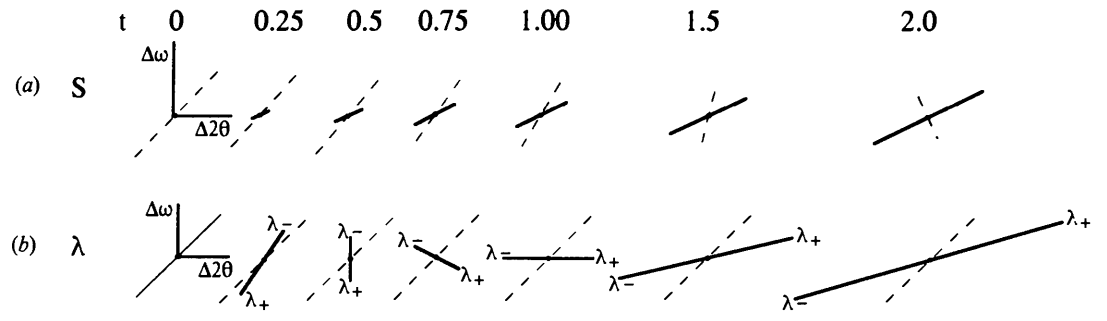

Fig. 2. For t values from 0 to 2.0, the distribution (solid line) and the locus of translation (dashed line) are shown respectively for (*a*) the source, *S*, and (*b*) the wavelength dispersion, λ.

The combination of these two components by multiplication yields a four-sided area, $a_{11}a_{21}a_{22}a_{12}$ (Fig. 1*a*), which we can designate, for brevity, MS.

The way in which the source distribution and its locus of translation change with t from 0 to 2.0 is shown in Fig. 2(*a*).

(*c*) *The mosaic spread of the monochromator crystal.* The line for zero mosaic spread, *i.e.* $\Delta\theta=0°$, in $\Delta\omega$, $\Delta 2\theta$ space is determined by the value of t (see *M*88, p. 1038). This line corresponds to the locus of translation of the mosaic spread. For $t=0.4$, this line is $L'0L''$ in Fig. 1(*b*). The mosaic spread is distributed about the line $L'0L''$ as in Fig. 1(*b*), being represented as a triangular distribution. Interaction of the mosaic-spread distribution with the previous result of combining the *M* and *S* distributions involves multiplication of MS by the mosaic-spread distribution, μ, to yield MSμ. If the triangular distribution extends to $\Delta_3\Delta_3$ (Fig. 1*b*), then the area of the shape is unchanged but the distribution within it is modified. If it extends only to $\Delta_2\Delta_2$, then the shape is reduced, becoming six-sided. Extended only to $\Delta_1\Delta_1$, the shape is further truncated to become four-sided but now is determined essentially by the monochromator length and its mosaic spread.

(*d*) *The wavelength distribution.* The usual source of neutrons involves 'white' radiation, so the wavelength distribution of the source is relatively broadly peaked, see *e.g.* Arndt & Willis (1966). Of this, only a limited band is passed by the monochromator to the specimen crystal and this is further modified by interaction with the wavelength dispersion of *c*. This has been dealt with in *M*88 and is summarized in diagram form in Fig. 2(*b*). It will be seen that the vector combination of the wavelength dispersion of *M* and of *c* leads to the total angular range of the wavelength band in $\Delta\omega$, $\Delta 2\theta$ space altering with change of t, first contracting and then expanding. Along $0'Z'_+$ (and $0''Z''_+$), it expands linearly with t. For $t=0.4$, the wavelength distribution and its locus of translation are shown in Fig. 1(*c*).

The combination of this fourth component, the wavelength distribution, λ, involves its multiplication with the previous three-component distribution, leading to either an unchanged area, a reduced area or, for a rather selective combination, an eight-sided shape (see Fig. 5 in *S*89).

Because, for $t=0.4$, the slope ($\sim 50°$) of the locus of translation of the source distribution in $\Delta\omega$, $\Delta 2\theta$ space does not differ greatly from the slope (45°) of the locus of translation of the wavelength distribution, the distinction between these two in this case is not readily demonstrated in a diagram.

So, we end up with a distribution for the apparatus function which is the *product* of the distributions of the four basic components. It may be noted that each additional component either leaves the *area* of the overall shape unchanged or truncates it to some extent. In no case is expansion of the area involved, a characteristic normally associated with the operation of convolution.

2. *The introduction of other components*

When one has to introduce further components to establish the shapes of Bragg reflections in a realistic experimental situation, it is necessary to consider with some care how such components are to be combined with the apparatus function.

In the case of the mosaic distribution, $\mu(\Delta\omega)$, of a real specimen crystal, each point on the distribution interacts with the apparatus function and superimposes with appropriate weight on the corresponding results from the series of other settings of $\Delta\omega$ on either side. The end result corresponds to the convolution of the apparatus function with the mosaic distribution.

For the physical size of the specimen crystal, the argument is a little more complicated and is dependent on the relative sizes of the specimen crystal and the monochromator. For the neutron case, the specimen crystals are of length of the order of 1–2 mm (say), whereas the monochromator crystal is likely to be of length 25 mm or greater. The distance between these will be of the order of 1.0–1.5 m. So the angle subtended by a 1 mm crystal at the centre of the monochromator will be of the order of 0.04–0.12°. The 'size' of the apparatus function in $\Delta\omega$, $\Delta 2\theta$ space is tied up with the angular aperture of the monochromator crystal at the specimen crystal, *c*. With the size of *M* viewed from *c* being 10–20 mm (depending on θ_M), this angular aperture is *ca* 0.4 to 1.2°. So the interaction of the apparatus function with the specimen crystal dimension corresponds to each point along the relevant dimension of the crystal interacting with a weight appropriate to that position (which will depend on the shape of the crystal and the reflecting power of that point) with the apparatus function as viewed from that point. Because of the relative aperture of the specimen crystal to that of the monochromator, the apparatus function as viewed from one end of the specimen crystal differs very little from that viewed from the other end so it is effectively constant. Under those circumstances, the appropriate mathematical operation is again convolution in two dimensions. As t changes, the combined shape involving the crystal dimension has the same locus in $\Delta\omega$, $\Delta 2\theta$ space as was deduced in Mathieson (1984*a*).

Illustration

Having shown in *M*88 and *S*89, with square and triangular functions, how the various factors can

specifically influence the outer limits of the shapes of reflections with change in t, we here demonstrate examples of the variation of the apparatus function and hence of reflection shapes with more realistic parameters.

With the dimensions for d_1 and d_2 given above, the source has a distribution that is flat-topped for 2.67 cm, with left and right edges composed of half-Gaussians each having a half-width at half-maximum of 0.67 cm (a total width at half maximum of 4.0 cm), and the wavelength distribution corresponded to a Gaussian peaking at 1.2 Å and of full width at half-maximum (FWHM) 0.65 Å. (The latter provides a reasonable substitute for a typical wavelength distribution because only the peak region is of significance for our present purpose.) The monochromator is 4 cm long with a d spacing that corresponds to a Bragg angle $\theta_M = 30°$ for $\lambda = 1.2$ Å and has a Gaussian mosaic spread with FWHM of 0.4°.

The resultant contoured calculated shapes of the apparatus function as it changes with θ_c are given in Fig. 3 for values of t from 0 to 1.0 in steps of 0.25 and then to 2.0 in a step of 0.5. Fig. 3(a) shows the shape for $t = 0.25$, while Fig. 3(b) provides a composite diagram where the reflection shapes for each t value are displaced along a slope of 1/2 with respect to the $\Delta 2\theta$ axis in such a manner as to stress the important role of the upper and lower bounds, $Z'_-0'Z'_+$ and $Z''_+0''Z''_-$ (not shown, but see Fig. 1a). The centre of each figure is at the origin of the particular shape. These shapes are in $\Delta\omega, \Delta 2\theta^{(0)}$ space, *i.e.* the detector is not stepped when $\Delta\omega$ is stepped, so it is equivalent to an ω scan. It is evident that, as t goes beyond 1.0, the shapes in $\Delta\omega, \Delta 2\theta$ space involve considerable elongation, mainly along the $\Delta 2\theta$ axis.

As has been shown previously (Mathieson, 1985), one can make the shape more compact, particularly for high t values (and indeed have an essentially constant $\Delta 2\theta$ width), by applying an affine transformation to the data to convert them to $\Delta\omega, \Delta 2\theta^{(2)}$ space, with the results shown in Fig. 4. In Fig. 4(a), the reflection shape for $t = 0.25$ is shown individually.

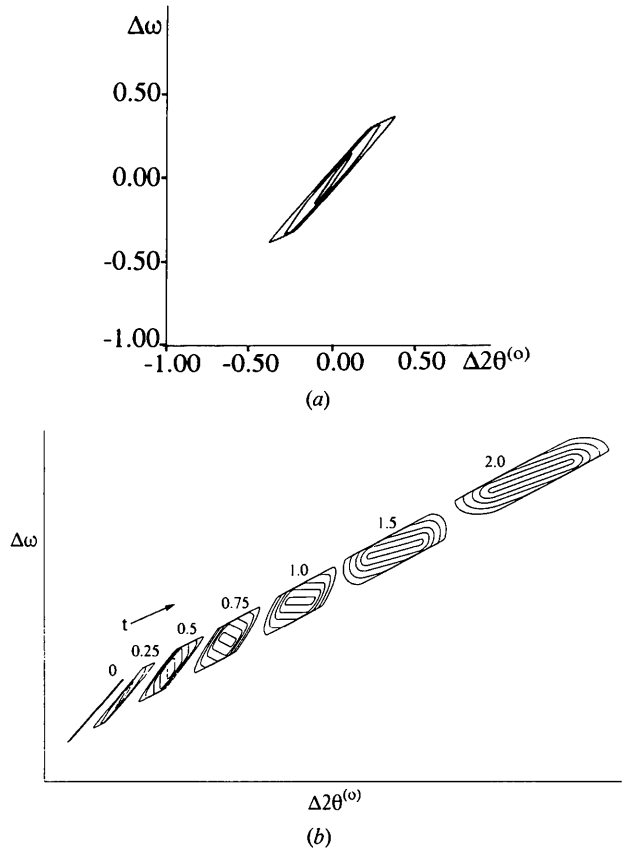

Fig. 3. Calculated shapes in $\Delta\omega, \Delta 2\theta^{(0)}$ space of the apparatus function, for (a) $t = 0.25$ contoured at three levels and (b) a composite of individual contoured shapes for $t = 0$ to 1.0 in steps of 0.25 and then 1.50 and 2.0, displaced along a slope of 1/2 with respect to the $\Delta 2\theta$ axis.

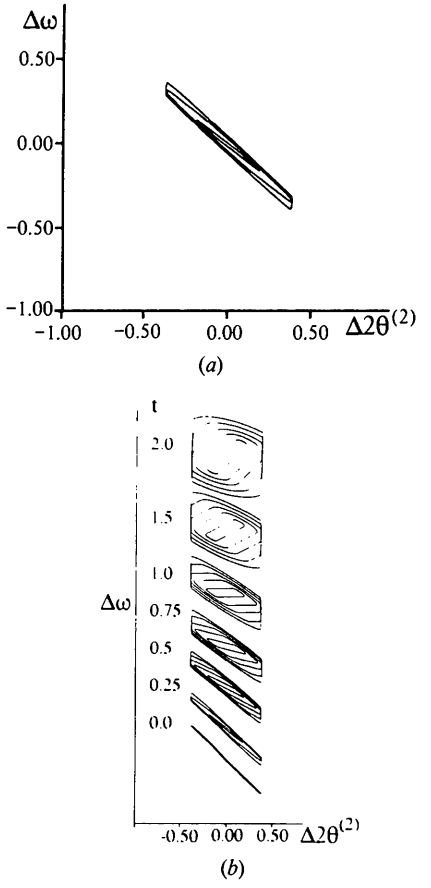

Fig. 4. Calculated shapes in $\Delta\omega, \Delta 2\theta^{(2)}$ space of the apparatus function, for (a) $t = 0.25$, contoured at three levels and (b) a composite of individual contoured shapes (reduced scale) for $t = 0$ to 1.0 in steps of 0.25 and then 1.50 and 2.0, displaced parallel to the $\Delta\omega$ axis.

Fig. 4(*b*) presents a composite diagram, but here the individual apparatus functions are displaced vertically, appropriate to the affine transformation for $s = 2$. In $\Delta\omega, \Delta 2\theta^{(2)}$ space, because of the compaction, the problem of where to establish the truncation contour between background and Bragg reflection is facilitated and hence the estimate of integrated intensity can be more reliable, *cf.* Figs. 3 and 4. In terms of practical operations, this end can be achieved without mathematical procedure by applying a step equal to $+2\Delta\omega$ to the detector for each $+\Delta\omega$ step of the crystal, *i.e.* by an ω–2θ-scan procedure.

Comparison of Figs. 3 and 4 makes it clear that treating the shape in $\Delta\omega, \Delta 2\theta^{(0)}$ space involves the need for more 'background' measurements than is the case for $\Delta\omega, \Delta 2\theta^{(2)}$ space.

Discussion

From the analysis above, we have arrived at the conclusion that, to simulate Bragg reflections in two-dimensional diffraction space, the components of the overall experimental arrangement fall into two groups; the components in one group being combined as a product and those in the second group by convolution.

By contrast, in the case of one-dimensional Bragg profiles (Alexander & Smith, 1962), all components were dealt with in the same way, being combined by convolution

The difference between the two-dimensional and one-dimensional cases can be indicated *via* the simpler nonmonochromator arrangement, which Alexander & Smith (1962) treated.

In $\Delta\omega, \Delta 2\theta$ space, following Mathieson (1982), we see that the components that contribute to the apparatus function consist of the source emissivity, σ, its wavelength distribution, λ, and an idealized specimen crystal, vanishingly small and with zero mosaic spread. The apparatus function is the *product* of the distributions, σ and λ. However, when this two-dimensional distribution is projected onto the $\Delta\omega$ axis to reproduce the one-dimensional profile (*cf.* Mathieson, 1984*b*, Fig. 6), it corresponds to the *one-dimensional convolution* of the projections on the $\Delta\omega$ axis of the individual σ and λ distributions.

When additional components associated with a realistic specimen crystal or detector system are involved, the combining operation is convolution. Hence, for the nonmonochromator one-dimensional-profile case, it turns out that the combining operation, whether in respect of the apparatus function or additional 'external' components, is the same.

When dealing with two-dimensional diffraction space, such as $\Delta\omega, \Delta 2\theta$ space, with or without a monochromator, the apparatus function is determined as a product. For the combination of 'external' components, such as the mosaic spread and dimension of a specimen crystal and the size of the detector aperture or the point-spread function of a gas-type, television-type or solid-state position-sensitive detector, the appropriate procedure is convolution.*

There is one significant advantage of the modelling approach compared with the setting-up of a library of reflection shapes (Wilkinson *et al.*, 1988). In the latter, because the shape of a Bragg reflection involves components other than the wavelength dispersion, there is considerable difficulty in establishing consistent empirical truncation limits as θ_c changes. In the former case, where the model shapes are synthesized by well defined functions, the truncation limits (which are presumed to define a definite ratio relative to the measure at infinity) need not be held constant but can be adjusted over the θ_c range. The appropriate normalizing factor can be established from the theoretical model (Mathieson, 1982).

Once established, the apparatus-function shapes hold until some change in the apparatus is made. In neutron diffraction, the apparatus function will generally be the major distribution determining the diffraction shape. Contributions from mosaic spread and specimen crystal size will probably be of minor weight (*cf.* Roth & Lewit-Bentley, 1982, p. 679).

APPENDIX

What we refer to as the 'apparatus function' differs significantly from what others refer to as the 'resolution function'. The difference arises from the choice of components to be included. Thus, for example, Cochran (1969), in treating the matter of the resolution function of a nonmonochromator case, includes, with the source and its wavelength distribution, the mosaic spread of the specimen crystal and also its size. In our analysis in two dimensions, we find that these latter components involve combining characteristics different from those of the former.

While it is evident that the source and the monochromator, as fixed components, must be included in the apparatus function, one must also recognize that, in order to ensure a homogeneous group of components in the apparatus function, it is necessary to include a dispersing agent, the specimen crystal, for completeness. However, a key point is that a diffractometer should ideally measure, in relation to a real specimen crystal, its (extinguished) reflectivity distribution [alias its mosaic spread; see Mathieson & Stevenson (1985) and Mathieson (1988*b*)]. So the specimen crystal included in the apparatus function must

* In situations where a monochromator is involved but its axis is perpendicular to that of the specimen crystal, the dispersions of M and c are at right angles so the situation is basically similar to the nonmonochromator case.

not involve the real characteristics of a specimen except its dispersion capability. The components associated with the real characteristics of the specimen crystal, namely the mosaic spread and its physical dimensions, must belong to a different group whose interactions are modelled by convolution.

We are grateful to Dr J. K. Mackenzie for extensive discussions on matters of convolution.

References

ALEXANDER, L. E. & SMITH, G. S. (1962). *Acta Cryst.* **15**, 983–1004.
ALLISON, S. K. & WILLIAMS, J. H. (1930). *Phys. Rev.* **35**, 149–154.
ARNDT, U. W. & WILLIS, B. T. M. (1966). *Single Crystal Diffractometry.* Cambridge Univ. Press.
COCHRAN, W. (1969). *Acta Cryst.* A**25**, 95–101.
CONVERT, P. & FORSYTH, J. B. (1983). Editors. *Position-Sensitive Detection of Thermal Neutrons.* London: Academic Press.
DENNE, W. A. (1977). *Acta Cryst.* A**33**, 438–440.
DUMOND, J. W. M. (1937). *Phys. Rev.* **52**, 872–883.
LEHMANN, M. S., KUHS, W. H., MCINTYRE, G. J., WILKINSON, C. & ALLIBON, J. R. (1989). *J. Appl. Cryst.* **22**, 562–568.
MATHIESON, A. MCL. (1982). *Acta Cryst.* A**38**, 378–387.
MATHIESON, A. MCL. (1983). *J. Appl. Cryst.* **16**, 257–258.
MATHIESON, A. MCL. (1984*a*). *J. Appl. Cryst.* **17**, 207–210.
MATHIESON, A. MCL. (1984*b*). *Acta Cryst.* A**40**, 355–363.
MATHIESON, A. MCL. (1985). *Acta Cryst.* A**41**, 309–316.
MATHIESON, A. MCL. (1988*a*). *Acta Cryst.* A**44**, 1036–1042.
MATHIESON, A. MCL. (1988*b*). *Aust. J. Phys.* **41**, 393–402.
MATHIESON, A. MCL. & STEVENSON, A. W. (1985). *Acta Cryst.* A**41**, 290–296.
ROTH, M. & LEWIT-BENTLEY, A. (1982). *Acta Cryst.* A**38**, 670–679.
SCHOENBORN, B. P. (1983). *Acta Cryst.* A**39**, 315–321.
SJÖLIN, L. & WLODAWER, A. (1981). *Acta Cryst.* A**37**, 594–604.
SPENCER, S. A. & KOSSIAKOFF, A. A. (1980). *J. Appl. Cryst.* **13**, 563–571.
STANSFIELD, R. F. D., THOMAS, M., MASON, S., NELMES, R. J., TIBBALLS, J. E. & ZHONG, W. L. (1983). In *Position-Sensitive Detection of Thermal Neutrons*, edited by P. CONVERT & J. B. FORSYTH, pp. 365–371. London: Academic Press.
STEVENSON, A. W. (1989). *Acta Cryst.* A**45**, 75–85.
WILKINSON, C., KHAMIS, H. M., STANSFIELD, R. F. D. & MCINTYRE, G. J. (1988). *J. Appl. Cryst.* **21**, 471–476.

Acta Cryst. (1993). A**49**, 661–667

Extinction Corrections from Equivalent Reflections

BY E. N. MASLEN AND N. SPADACCINI

Crystallography Centre, University of Western Australia, Nedlands, Western Australia 6009, *Australia*

(*Received* 1 *April* 1992; *accepted* 15 *February* 1993)

Abstract

Corrections for secondary extinction evaluated from the diffraction intensities for equivalent reflections with different path lengths provide an independent check on values that minimize differences between observed and calculated structure factors. Comparison of equivalent intensities also avoids any extinction-parameter bias, which originates in correlation of the extinction corrections with bonding-electron contributions to X-ray structure factors. Corrections from the comparison of equivalent reflections for several X-ray diffraction studies on small crystals of ionic compounds are markedly less than those that minimize differences between observed and calculated structure factors. The discrepancies that originate in extinction-parameter bias are exacerbated by the unfavourable form of the statistical distribution function for the residuals when differences between observed and calculated structure factors are minimized. Analysis of intensities for equivalent reflections, although more demanding experimentally, provides least-squares residuals closer to the normal distribution required for reliability in nonlinear least-squares processes.

Introduction

The kinematic theory of diffraction, readily derived from the first Born approximation, assumes that the radiation is diffracted no more than once in a crystal. At the Bragg condition, the diffracted beam is necessarily oriented so that second- and higher-order elastic coherent scattering occurs. Kinematic theory assumes the scattering contributions to be so small that second- and higher-order processes can be neglected. This assumption is valid and accurate for weak reflections from small crystals. In principle, measured structure factors for stronger reflections may be corrected for high-order components to the scattering by perturbation techniques, if kinematic theory is obeyed approximately.

Estimates of extinction corrections independent of any structural model have been reported for crystals in the form of large slabs cut parallel to a desired